AD-A191 868 CHARACTERIZATION OF SPARK EROSION OF METAL ALLOYS(U) 1/1
NAVAL OCEAN SYSTEMS CENTER SAN DIEGO CA W E GLAD
AUG 86 NOSC/TR-1140

UNCLASSIFIED F/G 11/6.1 NL

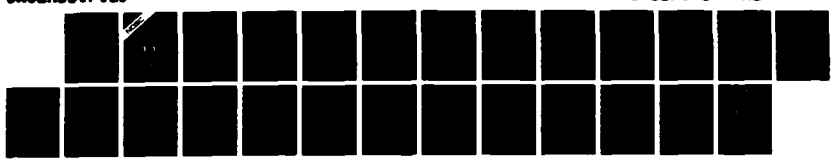

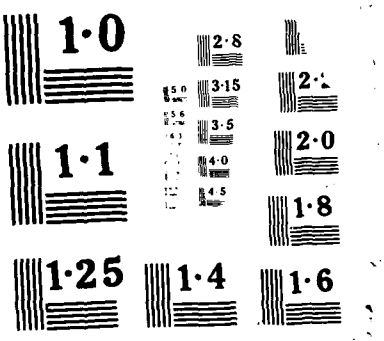
1·0
1·1
1·25
2·8
3·15
3·5
4·0
4·5
2·0
1·8
1·4
1·6

NOSC TR 1148

NAVAL OCEAN SYSTEMS CENTER San Diego, California 92152-5000

NOSC TR 1148

Technical Report 1148
August 1986

Characterization of Spark Erosion of Metal Alloys

W. E. Glad

NAVAL OCEAN SYSTEMS CENTER

San Diego, California 92152-5000

E. G. SCHWEIZER, CAPT, USN
Commander

R. M. HILLYER
Technical Director

ADMINISTRATIVE INFORMATION

The work reported here was performed by members of the Structural Materials Science Branch, Design and Development Division, with funding provided by the Director of the Navy Laboratories (DNL), Independent Research Programs (IR), Washington, DC 20360. Local coordination was provided by E.P. Cooper, Program Director for Research, Naval Ocean Systems Center.

Released by
R.K. Fogg, Jr., Head
Structural Materials
Science Branch

Under authority of
C.L. Ward, Jr., Head
Design and Development
Division

RH

UNCLASSIFIED
SECURITY CLASSIFICATION OF THIS PAGE

REPORT DOCUMENTATION PAGE

AD-A191 060

1a REPORT SECURITY CLASSIFICATION UNCLASSIFIED	1b RESTRICTIVE MARKINGS
2a SECURITY CLASSIFICATION AUTHORITY	3 DISTRIBUTION/AVAILABILITY OF REPORT Approved for public release; distribution is unlimited.
2b DECLASSIFICATION/DOWNGRADING SCHEDULE	
4 PERFORMING ORGANIZATION REPORT NUMBER(S) NOSC TR 1148	5 MONITORING ORGANIZATION REPORT NUMBER(S)
6a NAME OF PERFORMING ORGANIZATION Naval Ocean Systems Center	6b OFFICE SYMBOL (if applicable) Code 932
6c ADDRESS (City, State and ZIP Code) San Diego, CA 92152-5000	7a NAME OF MONITORING ORGANIZATION 7b ADDRESS (City, State and ZIP Code)
8a NAME OF FUNDING/SPONSORING ORGANIZATION Director of Navy Laboratories Independent Research Programs	8b OFFICE SYMBOL (if applicable) DNL, IR
8c ADDRESS (City, State and ZIP Code) Washington, DC 20360	9 PROCUREMENT INSTRUMENT IDENTIFICATION NUMBER 10 SOURCE OF FUNDING NUMBERS

PROGRAM ELEMENT NO	PROJECT NO	TASK NO	AGENCY ACCESSION NO
61152N	RR0001	RR0000101	DN306 227

11 TITLE (Include Security Classification)
Characterization of Spark Erosion of Metal Alloys

12 PERSONAL AUTHOR(S)
W. E. Glad

13a TYPE OF REPORT	13b TIME COVERED	14 DATE OF REPORT (Year, Month, Day)	15 PAGE COUNT
Final	FROM _____ TO _____	August 1986	25

16 SUPPLEMENTARY NOTATION

17 COSATI CODES			18 SUBJECT TERMS (Continue on reverse if necessary and identify by block number)
FIELD	GROUP	SUB GROUP	Physical chemistry, inorganic chemistry, metallurgy and metallography metal alloys, spark erosion, spark emission analysis, conductive solids nebulization (CSN), inductively coupled plasma (ICP) optical emission spectroscopy

19 ABSTRACT (Continue on reverse if necessary and identify by block number)

A new spectroscopic emission technique, inductively coupled plasma (ICP) optical emission spectroscopy, in conjunction with spark erosion or conductive solids nebulization (CSN), was used in obtaining rapid elemental analysis of metal alloys. Enthalpies of vaporization were shown not to be the determining factor in the amount of material eroded in medium-voltage sparks. The melting behavior of the alloys seems to have a more significant effect on the amount of material eroded. Perhaps, instead of direct vaporization, the mechanism of erosion involves the mechanical sputtering of molten metal into the aerosol. However, in a standard spark source, for which both erosion and excitation occur simultaneously, the sample eventually must be vaporized to give an atomic emission signal. While it might be expected that melting would not play such a significant role for standard spark sources as the CSN-ICP measurements described here would indicate, comparative measurements of iron emission signals from iron-nickel and iron-chromium alloys, using a standard spark system, yield results similar to those observed in this work: the chromium alloys show much less iron intensity than nickel alloys with the same iron concentration. The important factor may be the amount of material present in the discharge gap, where vaporization and excitation take place. The sputtering of material into the gap, and thus a melting behavior, would then be important even in a standard spark stand. Copper-zinc alloy results show that effects other than melting behavior must be important for aerosol generation, but the identity of these effects could not be determined. The results of the CSN-ICP stainless steel calibration indicate that, even though the causes of variation in the amount of material eroded are not completely understood, they can be corrected by a simple intensity ratio and matrix dilution calculation procedure when linear curves are produced. The calibration yielded superior analysis results for the main elements of stainless steels of widely varying composition.

20 DISTRIBUTION/AVAILABILITY OF ABSTRACT	21 ABSTRACT SECURITY CLASSIFICATION
☐ UNCLASSIFIED/UNLIMITED ☒ SAME AS RPT ☐ DTIC USERS	UNCLASSIFIED

22a NAME OF RESPONSIBLE INDIVIDUAL	22b TELEPHONE (Include Area Code)	22c OFFICE SYMBOL
W. E. Glad	(619) 553-3223	Code 932

DD FORM 1473, 84 JAN

83 APR EDITION MAY BE USED UNTIL EXHAUSTED
ALL OTHER EDITIONS ARE OBSOLETE

UNCLASSIFIED
SECURITY CLASSIFICATION OF THIS PAGE

DD FORM 1473, 84 JAN

EXECUTIVE SUMMARY

PROBLEM

Investigate the use of the new spectroscopic emission technique, inductively coupled plasma (ICP) optical emission spectroscopy, in conjunction with spark erosion of conductive solids nebulization (CSN), in obtaining rapid elemental analysis of metal alloys.

RESULTS

Enthalpies of vaporization were shown not to be the determining factor in the amount of material eroded in medium-voltage sparks. The melting behavior of the alloys seems to have a more significant effect on the amount of material eroded. Perhaps, instead of direct vaporization, the mechanism of erosion involves the mechanical sputtering of molten metal into the aerosol. However, in a standard spark source, for which both erosion and excitation occur simultaneously, the sample eventually must be vaporized to give an atomic emission signal. While it might be expected that melting would not play such a significant role for standard spark sources as the CSN-ICP measurements reported here would indicate, comparative measurements of iron emission signals from iron-nickel and iron-chromium alloys, using a standard spark system, yield results similar to those observed in this work: the chromium alloys show much less iron intensity than nickel alloys with the same iron concentration. The important factor may be the amount of material present in the discharge gap, where vaporization and excitation take place. The sputtering of material into the gap, and thus the melting behavior, would then be important even in a standard spark stand. Copper-zinc alloy results show that effects other than melting behavior must be important for aerosol generation, but the identity of these effects could not be determined. The results of the CSN-ICP stainless steel calibration indicate that, even though the causes of variation in the amount of material eroded are not completely understood, they can be corrected by a simple intensity ratio and matrix dilution calculation procedure when linear curves are produced. The calibration yielded superior analysis results for the main elements of stainless steels of widely varying composition.

RECOMMENDATION

The use of CSN-ICP for the examination of highly alloyed materials, rather than standard spark analysis equipment, is recommended.

CONTENTS

FIGURES

TABLES

INTRODUCTION

Spark emission analysis has been used for many years to obtain rapid elemental analysis of metal alloys. The general principles of the technique are straightforward. A medium- to high-voltage spark is used to volatize, atomize, and excite the sample to emit visible and ultraviolet light. Since atoms emit light at discrete wavelengths (commonly called "emission lines") characteristic of the atomic species present, it is possible to disperse the wavelengths with a grating and detect light emitted by specific elements. If a calibration relationship can be established between the intensity of the light at a given wavelength and the concentration of an element in an alloy sample, the alloy can be analyzed quantitatively for that element.

There are a number of factors that affect the calibration behavior of an atomic emission line. These include variation in sample volatization, self-absorbtion of emitted radiation by 'cold' atoms in the discharge plasma, and interference from coincident or adjacent atomic lines from other elements. Consequently, calibration of spark instruments for quantitative analysis is an empirical process. Usually, a different set of calibration curves is generated for each alloy type to be analyzed. This results in considerable expense in operator time and training, and requires a large number of different (and expensive) standard reference materials. The operator must be vigilant to be sure that the calibration standards he is using match the sample being analyzed; otherwise, inaccurate analyses will result. In some cases, particularly for highly alloyed metals in which the concentrations of alloying elements can vary widely, it is impossible to generate acceptable calibrations. It is suspected that the difficulty encountered in analyzing highly alloyed metals is caused because changing the content of the alloying elements in a metal alloy drastically changes the amount of sample that is volatized.

Recently, a new spectroscopic emission technique, inductively coupled plasma (ICP) optical emission spectroscopy, has become popular. The ICP is generated in a stream of argon gas that is ionized by an induction field set up by a coil surrounding the quartz torch that channels the argon stream. The sample is introduced up the central axis of the cylindrical torch and is excited to emit light by the plasma. Because the sample is excited in the center of the plasma, the light source is optically thin and produces very linear calibration curves. In addition, the ICP operates at a temperature that is high enough (5000–10000 K) to produce atoms of even refractory materials. Usually, the sample is introduced into the ICP as a liquid solution. This can sometimes be a limitation for the analysis of metal alloys, since it can be difficult to completely dissolve some metal alloys. Furthermore, the dissolution step is usually time-consuming and susceptible to errors.

In the last few years, a technique has been developed to introduce metal samples to the ICP in a more convenient manner. The method is called spark erosion or conductive solid nebulization (CSN). This method employs a spark source to erode material from the alloy and produce an aerosol that is introduced into the plasma. This avoids the sample dissolution step in ICP analysis, yet still allows the use of the favorable properties of the ICP as an emission source. It is a particularly interesting method of analysis because the generation of aerosol is separate from the excitation process. It is thus possible to separate complicating effects in the aerosol generation from those in the excitation.

Since the CSN is really just a classical spark source connected to a very linear elemental detector, it provides an excellent method to study the properties of sample erosion caused by the spark source. The sample erosion properties of several alloys are examined here with CSN-ICP. An attempt is made to correlate, at least qualitatively, this erosion behavior with the physical properties of the alloy. Results from an actual analytical calibration using CSN-ICP are given to illustrate a simple method of correction for variations in sample erosion.

EXPERIMENTAL SETUP

SPECTROMETER

The spectrometer used was an Applied Research Laboratories 3580. The optical properties of this instrument are described in an earlier report.[1] The plasma torch was operated with 1200 watts of incident power. Reflected power was less than five watts when aqueous solutions were introduced with a nebulizer of the pneumatic concentric type. When aerosol from the CSN was introduced to the torch, the reflected power ran at about 15 watts.

The CSN was also manufactured by Applied Research Laboratories. A simple schematic of the principle involved is shown in figure 1. The CSN consists of a spark source and a spark analysis table. Argon gas passes through the table and sweeps the aerosol that is generated by spark activity through a length of ¼-inch plastic tubing into the plasma torch. When the CSN is used, the torch is connected to this tubing instead of to the normal liquids spray chamber. Because no water is introduced into the torch when the CSN is used, the torch temperature is slightly different from that of normal liquids operation, and no OH molecular emission bands are present in the spectrum.

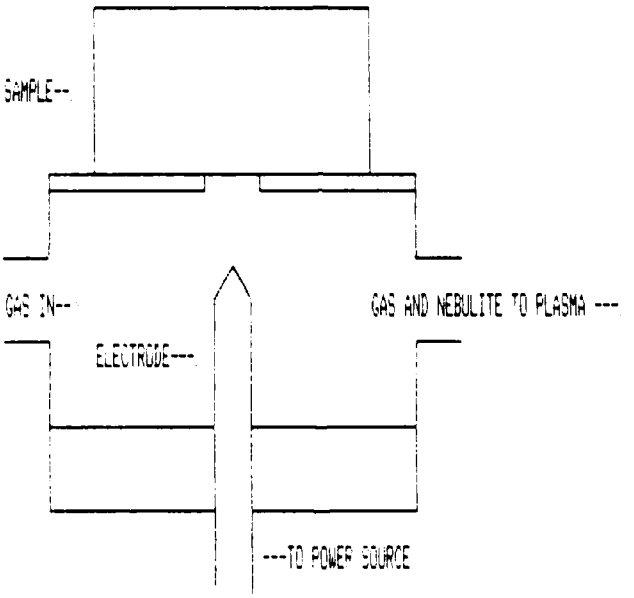

Figure 1. Schematic of the sampling arrangement for the CSN.

When the CSN is used for spectrochemical analysis, the procedure is to first purge the system for 5 seconds with a 12 ℓ min flow of argon. The sample is then presparked for 20 seconds with the argon flow reduced to 5 ℓ min. Finally, the source conditions are changed and the argon flow reduced again to 1 ℓ min while signals are integrated. A rough schematic of the sparking circuit is shown in figure 2. The capacitor C is charged to a preset voltage by the charging circuit. When the capacitor is fully charged, a high voltage (17-kV) spark ionizes a path to the sample and the capacitor discharges through L and R to attack the sample. This charge and discharge cycle takes place at 120 Hz. The capacitor value is fixed at 10 μF. During presparking, L = 20 μH and R is removed from the circuit. The capacitor is charged to 500 V

for iron, nickel, and copper-base materials, and 350 V for aluminum. The purpose of presparking is to melt and homogenize the sample surface. The conditions are thus chosen to provide a high discharge current. During integration, L = 120 μH, R = 2.2 Ω, and the capacitor is charged to 400 V for iron, copper, and nickel bases, and 350 V for aluminum. Under integration conditions, the resulting spark current is essentially a semisinusoidal pulse of about 0.5-ms duration. When the capacitor is charged to 400 V, the peak current in the pulse is about 60 A. Because R is larger than the resistance of the samples (which are typically a few tenths of an ohm), the current provided during integration is essentially constant, and independent of the sample. Consequently, the energy expended in the discharge gap remains relatively constant.

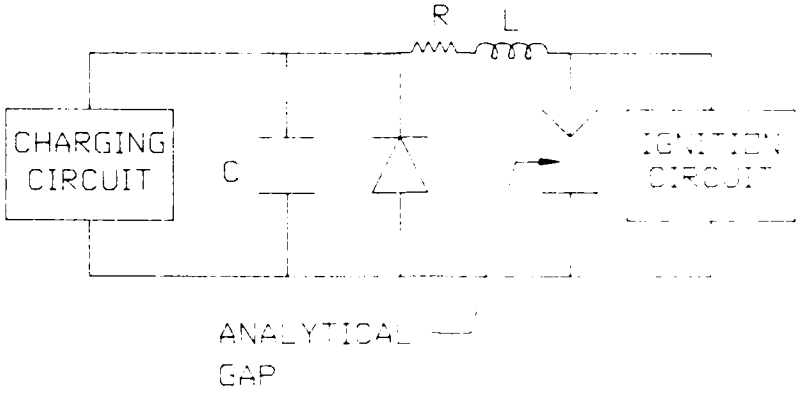

Figure 2. Rough schematic of the CSN sparking circuit.

STANDARDS

Copper-base binary standards were obtained from BNF Metals Technology Center of Wantage, England. Chromium-iron binaries and nickel-iron binaries were obtained from SKF Steel, Sweden, and the Research Institute of Siderurgie, France. (Iron-cobalt binaries were also from the Research Institute of Siderurgie.) Stainless steel standards for analytical calibration were from the National Bureau of Standards and the Brammer Standard Company, Inc., of Houston, Texas.

AEROSOL COLLECTION

Aerosol that was generated by the CSN was collected as shown in figure 3. During the purge and prespark cycles, the valve was set to vent the aerosol to the room. During the integration cycle, the valve was switched to direct the aerosol into the filter assembly where the aerosol was collected on the filters. The filters used were 25 mm in diameter and made of glass fibers. The purge time was 5 seconds, the prespark 20 seconds, and the integration time was 30 seconds. For copper-base materials, the valve was solenoid-controlled to switch when the integration cycle started. It was found that the solenoid valve interfered with the transfer of ferrous material, so for iron-nickel binaries, the solenoid valve was replaced with a hand-operated valve.

For each sample examined, three filters were collected. All three filters were put in a Teflon beaker and the aerosol was dissolved in acid and taken to a final volume of 25.0 ml. For iron-nickel binaries, 1 ml of concentrated nitric and 1 ml of concentrated phosphoric acid was used. Copper-base materials were dissolved with 2 ml of concentrated nitric acid. The solutions

obtained were then analyzed by using conventional-liquids ICP. To account for impurities already present in the filters, a blank consisting of three clean filters was also subjected to the same procedure for each collection run.

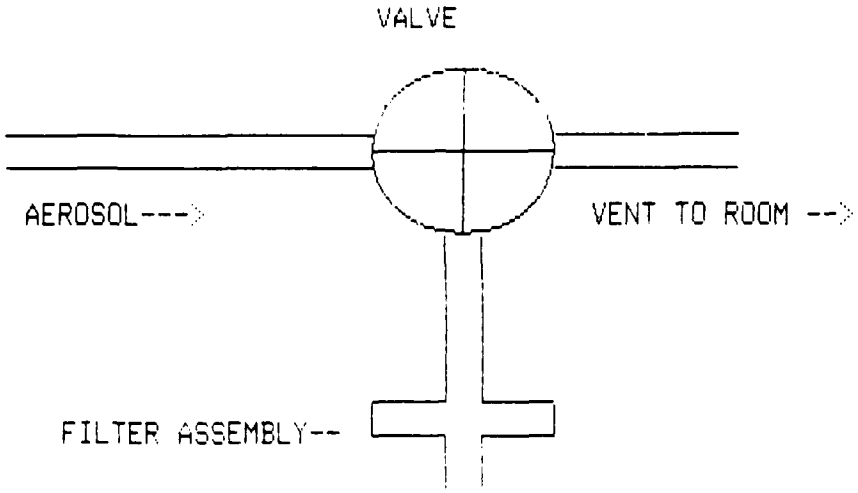

Figure 3. Aerosol collection arrangement

INTENSITY MEASUREMENTS

For intensity measurements, the output of the CSN was connected to the plasma torch. After the lines were purged with 12-ℓ min argon for 5 seconds, samples were subjected to a 20-s prespark. Intensities were then integrated for 5 s by using the readout electronics of the spectrometer. The intensities reported were an average of at least three runs. Relative standard deviations for the intensity measurements were usually 2% or less. Table I shows the emission lines that were used for intensity measurements. The Fe-273.96-nm line was used for iron-cobalt binaries because of a cobalt interference on the more commonly used Fe-271.44-nm line.

Table 1. Emission wavelengths.

Copper base

Element	Wavelength (nm)
Cu	224.26
Zn	330.25
SN	189.98

Iron base:

Element	Wavelength (nm)
Ni	243.49
Cr	298.92
Co	258.03
Fe (Cr and Ni work)	271.44
Fe (Co work)	273.96

Stainless Steel

Element	Wavelength (nm)
Fe	271.44
C	193.90
Mn	293.31
P	178.29
S	180.73
Si	212.41
Cu	327.4
Cr	298.9
V	311.07
Mo	202.03
Co	228.62
Nb	319.5
Se	196.09
Cu	224.26
Ni	2[illegible]60
Ti	342.26

RESULTS AND DISCUSSION

AEROSOL COLLECTION

The results of aerosol collection experiments and CSN intensity measurements for a set of copper-zinc and a set of iron-nickel binary alloy standards are given in table 2. The 18.4 ppm of iron found in the collection solution from National Bureau of Standards 1265 (an electrolytic iron standard, 99.9% pure iron) corresponds to a sample erosion rate of 5.1 μg s. During normal liquids ICP, a 0.5% metal solution is aspirated at 2.5 mℓ min. Assuming a 1% sample nebulization efficiency (which is typical for the type of nebulizer used), this would correspond to an injection rate of 2.1 μg s of metal to the torch. Earlier work[1] has shown that, for steels, the signal intensities from CSN injection are about five times greater than those from liquids injection of a 0.5% metals solution. For these results to be consistent, either the liquids nebulization efficiency is less than 1% or some of the increased intensity observed with the CSN is the result of increased torch temperature. A comparison of the intensity of argon 418.19-nm and 419.83-nm emission lines with and without liquids injection shows that the intensity of the argon lines decreases by more than a factor of two when liquid is injected. This suggests that some of the increase in emission intensity observed with the CSN may well be the result of an increased torch temperature.

Table 2. Aerosol collection and emission intensity results.

COPPER-ZINC ALLOYS

Sample	Intensity (mV)	Cu found (ppm)	%Cu found	%Cu certified	Zn intensity (mV)	Zn found (ppm)	%Zn found	%Zn certified
1251	7945	12.8	99.29	99.90	4.96	0.091	0.71	0.00
3010	7057	13.39	94.45	95.32	98.1	0.79	5.55	4.68
3009	6339	11.73	88.7	90.20	187.7	1.50	11.31	9.80
3008	5950	10.73	84.4	85.15	281.2	1.98	15.6	14.84
3007	5631	9.57	78.0	79.82	382.97	2.70	22.0	20.18
3005	4918	8.60	70.0	70.01	526.33	3.69	30.01	28.70
3003	4145	6.91	58.51	59.01	741.1	4.90	41.5	40.19
3001	3811	6.32	53.3	53.80	873.1	5.54	46.7	46.2

IRON-NICKEL ALLOYS

Sample	Fe intensity (mV)	Fe found (ppm)	%Fe found	%Fe certified	Ni intensity (mV)	Ni found (ppm)	%Ni found	%Ni certified
1265	3756	18.4	99.6	99.99	10.4	0.07	0.40	0.000
21	3840	19.4	99.2	99.38	19.1	0.16	0.80	0.62
4H	4025	19.4	96.7	96.9	58.2	0.66	3.28	3.10
2C	3992	19.5	94.7	94.56	94.9	1.09	5.28	5.44
3G	3871	19.5	89.9	89.6	136.0	2.17	10.0	10.37
4A	3762	18.1	82.4	81.55	328	3.6	17.6	18.5
5Z	3732	18.1	78.9	77.99	407	4.85	21.1	22.0
87E	3967	19.7	71.5	69.9	649	7.84	28.5	30.1
88D	3353	16.65	61.5	60.0	866	10.41	38.5	40.0

Comparison of the percentage of zinc found in the aerosol with the percentage certified in the samples show that for all standards a higher percentage of zinc was found in the aerosol than was certified in the samples. While this might be expected, since zinc is more volatile than copper (the boiling point of zinc is 908°C versus 2547°C for copper), the difference is quite small, just larger than the experimental precision. In the iron-nickel alloys, a higher percentage of nickel was found in the aerosol at low nickel concentrations, but a lower percentage was found in the aerosol at high nickel concentrations. Again, the differences are small. Nickel is only slightly less volatile than iron (boiling point of 2902°C versus 2877°C for iron). The fairly close agreement between the composition of the sample and the composition of the aerosol was somewhat unexpected, particularly for the copper-zinc system. Because of the great difference in boiling points of copper and zinc, more fractional distillation of zinc was expected.

Plots of CSN signal intensity versus the concentrations of metal found in aerosol collections are given in figures 4, 5, 6, and 7. In general, it was found that the CSN intensity is reasonably well correlated with the amount and composition of the aerosol eroded. Figure 8 shows a plot of the "normalized" emission intensity of the matrix element versus the total amount of metal collected for the iron-nickel alloys. The normalized intensity is defined as 100 times the measured emission intensity of the matrix element in the sample, divided by the product of the emission intensity of a sample of the pure matrix element and the fraction of the matrix element in the sample. Thus the normalized intensity of a pure iron sample is defined to be 100. No evidence of any major nonlinearity or self-absorbtion of the emission lines is observed. Thus the normalized emission intensity, as defined above, appears to be a reasonably good measure of the amount of material eroded from the sample.

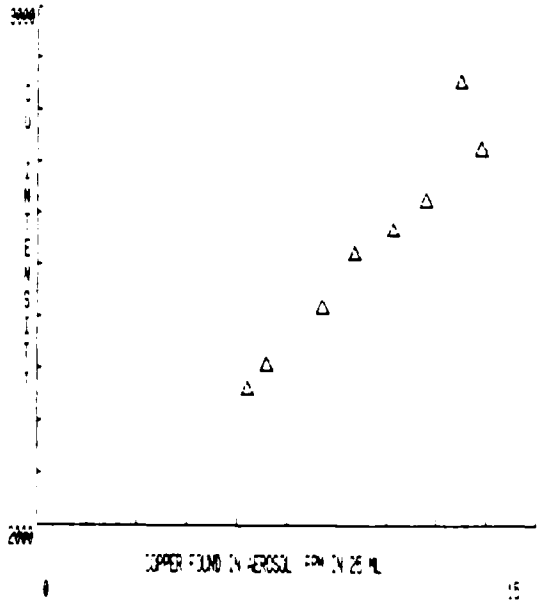

Figure 4 CSN emission intensity from Cu-224-nm line versus copper content of aerosol collections for some copper-zinc alloys.

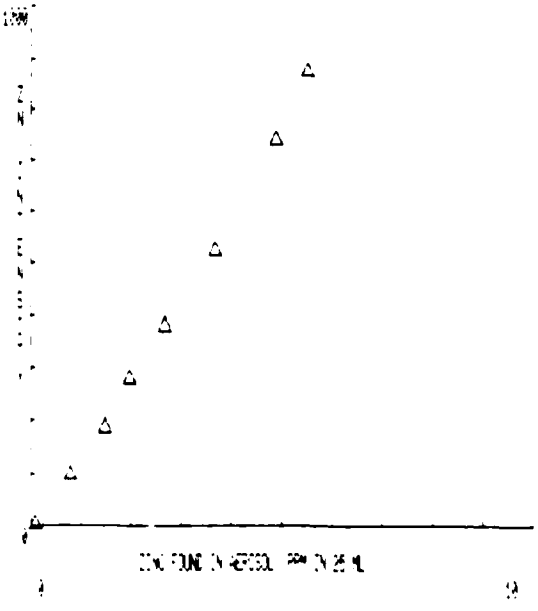

Figure 5 CSN emission intensity from Zn 330 nm line versus zinc content of aerosol collections for some copper-zinc alloys

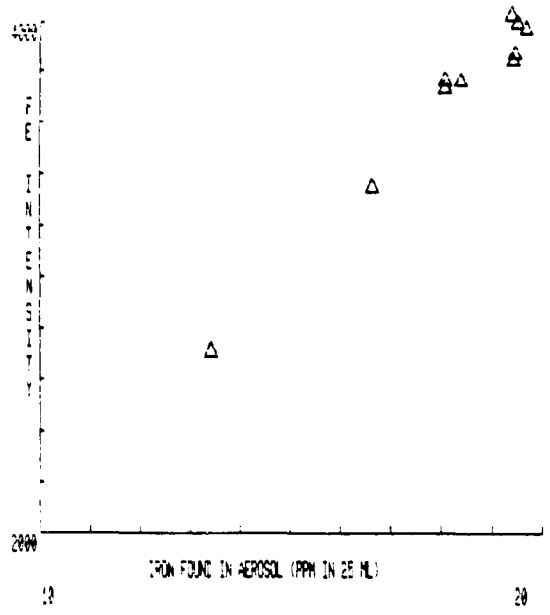

Figure 6. CSN emission intensity from Fe-271-nm line versus iron content of aerosol collections for some iron-nickel alloys.

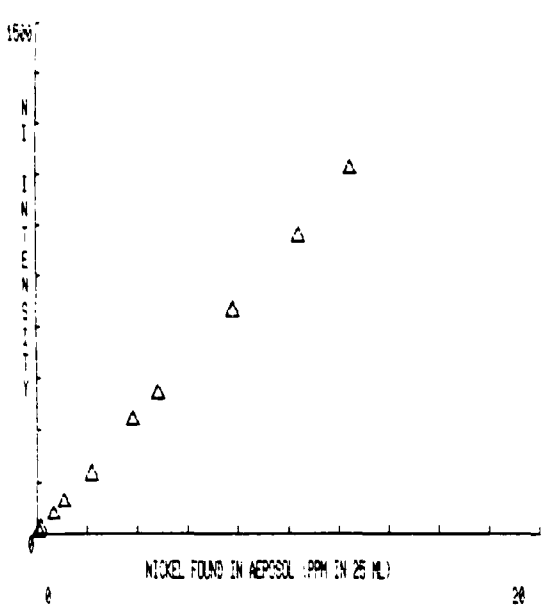

Figure 7. CSN emission intensity from Ni-243-nm line versus nickel content of aerosol collections for some iron-nickel alloys.

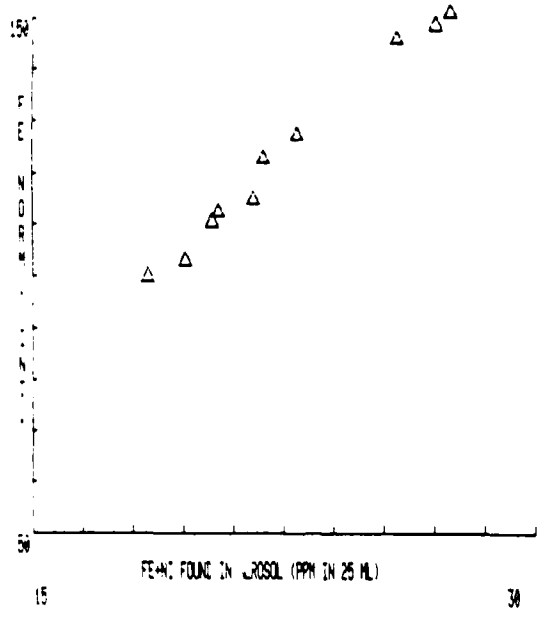

Figure 8. Normalized intensity of Fe-271-nm line versus iron plus nickel content of aerosol collections for some iron-nickel alloys.

CSN MEASUREMENTS

In addition to CSN intensity measurements on the copper-zinc and iron-nickel binary alloys, measurements were also made for iron-chromium, iron-cobalt, and copper-tin alloys. Figures 9 through 13 give plots of the normalized emission intensity of the matrix element versus the alloying element concentration. If equal amounts of material were eroded from all samples of a given alloys type, all of the plots in figures 9 through 13 would be horizontal lines. This is clearly not the case. All of the alloy systems studied here show significant variations of the normalized emission intensity of the matrix element with composition.

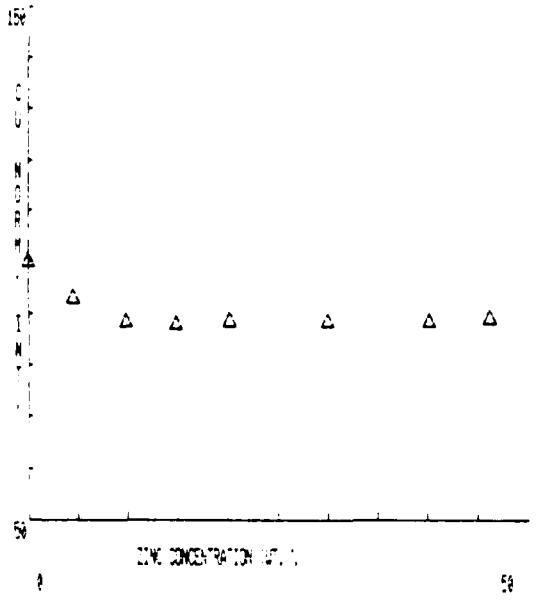

Figure 9 Normalized intensity of Cu-224-nm line versus zinc concentration for some copper-zinc alloys.

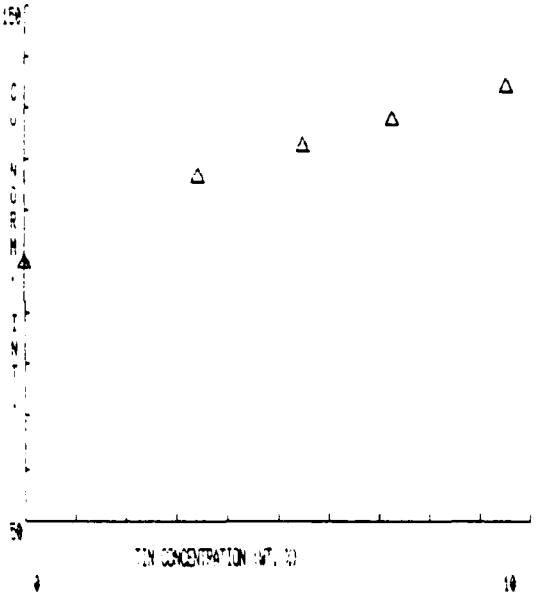

Figure 10. Normalized intensity of Cu-224-nm line versus tin concentration for some copper-tin alloys.

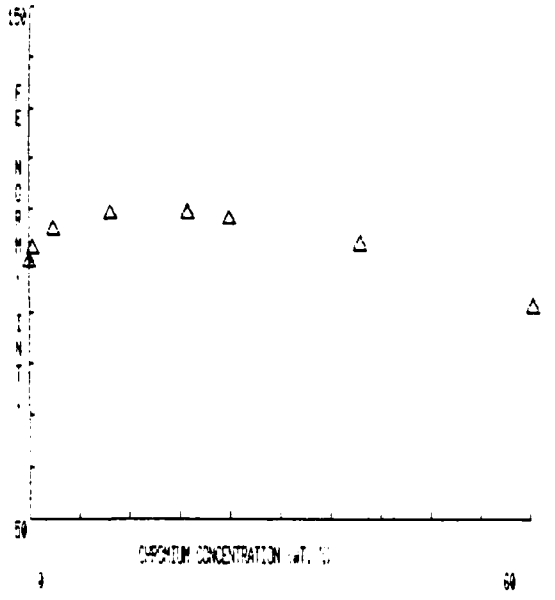

Figure 11. Normalized intensity of Fe-271-nm line versus chromium concentration for some iron-chromium alloys.

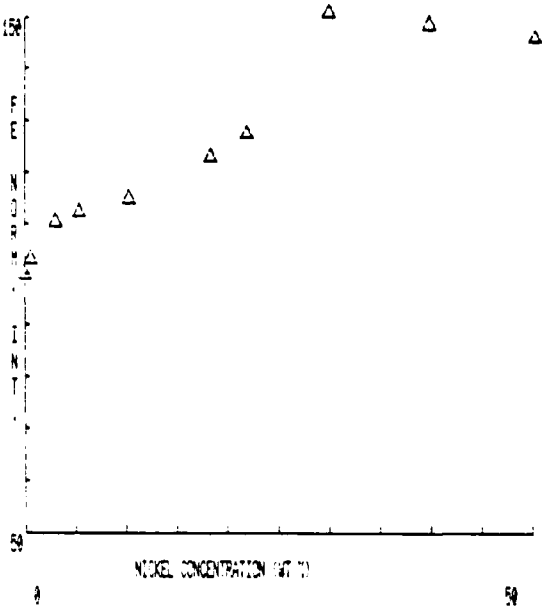

Figure 12. Normalized intensity of Fe-271-nm line versus nickel concentration for some iron-nickel alloys.

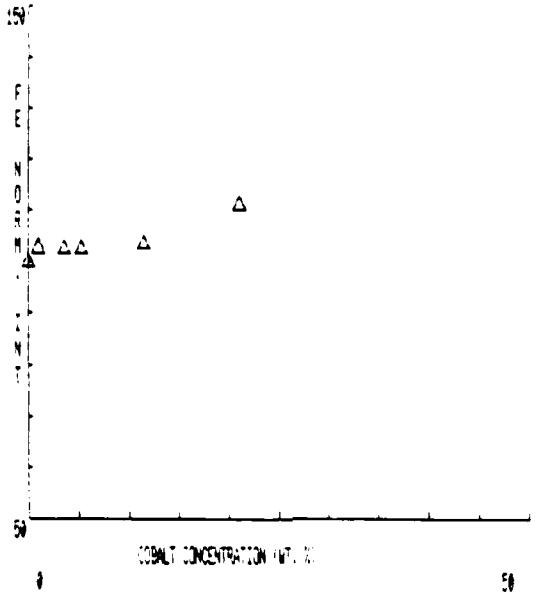

Figure 13 Normalized intensity of Fe-273-nm line versus cobalt concentration for some iron-cobalt alloys

One possible explanation for the variation of the amount of material eroded with alloying is that alloying affects the enthalpy of vaporization of the sample. If the amount of energy expended in the spark gap is constant, then samples with lower vaporization enthalpies would be more easily eroded. Vaporization enthalpy information as a function of alloy composition is scarce in the literature. However, the vaporization process for an alloy can be broken into elementary steps.

For an alloy containing metals A and B, with x the mole fraction of B:

Reaction	Enthalpy term
$A_{1-x}B_x(s) \rightarrow (1-x)A(s) + xB(s)$	$-\Delta H_{mix}$
$(1-x)A(s) + xB(s) \rightarrow (1-x)A(g) + xB(g)$	$(1-x)\Delta H_{vap}(A) + x\Delta H_{vap}(B)$
$A_{1-x}B_x(s) \rightarrow (1-x)A(g) + xB(g)$	$-\Delta H_{mix} + (1-x)\Delta H_{vap}(A) + x\Delta H_{vap}(B)$

where $\Delta H_{vap}(A)$ and $\Delta H_{vap}(B)$ are the vaporization enthalpies of pure A and B, respectively, and ΔH_{mix} is the enthalpy of mixing of A and B for the given composition. The enthalpy of vaporization of the alloy can be broken into the sum of the vaporization enthalpies of the individual elements (multiplied by the appropriate mole fraction) and the opposite of the enthalpy of mixing. Values of ΔH_{mix} are available for most binary alloys at some temperature[2] and vaporization enthalpies of pure metals are well tabulated. Compared to the vaporization enthalpies, which run from 30–120 kcal/g-atom for the metals considered here, the enthalpies of mixing are small, ranging from about −2 to +2 kcal/g-atom for the metal alloys considered here. For our purposes, it is thus not a bad approximation to assume that

$$\Delta H_{vap}(\text{alloy } A_{1-x}B_x) \approx (1-x)\Delta H_{vap}(A) + x\Delta H_{vap}(B)$$

Table 3 gives values of the vaporization enthalpy calculated in this manner for copper-zinc, copper-tin, iron-nickel, and iron-chromium alloys. The small changes in vaporization enthalpy for the copper-tin system cannot account for the large changes in normalized emission intensity that are observed in figure 10. Furthermore, the vaporization enthalpies of the more highly alloyed copper-zinc alloys are much smaller than the vaporization enthalpy of the 9.5% copper-tin alloy, yet the copper-tin alloy shows nearly 40% more normalized intensity. There is very little difference between the vaporization enthalpies of the iron-chromium and iron-nickel alloys systems over any of the concentration ranges studied, yet there are significant differences in the normalized intensities. These results suggest that vaporization enthalpy is not a significant factor in determining the amount of material eroded from samples.

A more significant factor in determining the amounts of material eroded seems to be the melting point of the material. This is best illustrated by the iron-chromium alloy system. Iron melts at 1538° C, while chromium melts at 1890° C. Examination of the phase diagram for this system[2] shows that, on the addition of chromium to pure iron, the melting temperature declines until it reaches a minimum at 22% chromium (1507° C), then increases towards the melting temperature of pure chromium. Examination of figure 11 shows that the amount of sample eroded mirrors this behavior. On the addition of chromium to pure iron, more material is eroded until a maximum is reached between 10% and 20% chromium, whereupon the

Table 3. Vaporization enthalpies.

Copper-zinc alloys

mole fraction Zn	ΔH_{vap} (kcal/g-atom)
0.0	80
0.1	75
0.2	71
0.3	66
0.4	61
0.5	56

Copper-tin alloys

mole fraction Sn	ΔH_{vap} (kcal/g-atom)
0.0	80.5
0.1	80
0.2	79
0.3	78

Iron-nickel alloys

mole fraction Ni	ΔH_{vap} (kcal/g-atom)
0.0	100
0.1	100
0.2	100
0.3	101
0.4	101
0.5	101

Iron-chromium alloys

mole fraction Cr	ΔH_{vap} (kcal/g-atom)
0.0	100
0.1	100
0.3	100
0.4	100
0.5	101

amount eroded decreases steadily. The normalized intensity data from the iron-nickel system does not mirror the melting-point behavior as well as the copper-tin system, but the gross features of the data indicate that melting behavior is important there as well. The melting point of iron-nickel mixtures decreases as nickel is added from the melting point of pure iron to a minimum near 65% nickel.[2] The normalized intensities in figure 12 increase steadily up to 30% nickel and then decrease slightly as the nickel content is increased to above 80%. The iron-cobalt data are also generally consistent with an increase in normalized intensity with decreasing melting point, although samples were available for measurement only up to 25% cobalt. The minimum melting point for the iron-cobalt system occurs near 60% cobalt.[2]

The normalized intensity from copper-tin alloys increases strongly as the percentage of tin in the sample is increased (figure 10). The amount of sample eroded clearly increases as the melting point decreases. The 9.5% tin sample has 34% more normalized intensity than the pure copper sample. Melting for the 9.5% tin sample begins at about 830 °C and ends at about 1010 °C, while pure copper melts at 1085 °C. However, the situation is different for copper-zinc alloys. As zinc is added to copper, the normalized intensity (figure 9) decreases slightly and levels out at about 90% of the normalized intensity of pure copper. This is true even at 46% zinc, where the melting point has decreased to about 980 °C. Obviously, there is a factor other than melting temperature that is important here.

Other properties that may affect the quantity of aerosol generated are the heat capacities and thermal conductivities of the samples, since, prior to melting or vaporizing, the samples must be heated in the solid state. The heat capacities will obviously affect the rate of heating. The thermal conductivities are important because the rate of heat conduction away from the point of spark attack will affect the temperature there and thus affect the erosion rate. In addition, the temperature at the sample surface close to the sites of spark attack may affect the recondensation rate of the aerosol. Unfortunately, neither of these properties can explain the difference in sample erosion behavior observed between the copper-tin and copper-zinc alloys.

STAINLESS STEEL CALIBRATION

Figure 14 shows normalized intensities as a function of the iron concentration for a number of stainless steel standards. Among the standards were ferritic, martensitic, and austenitic types. It can be seen that the amounts of material eroded varied considerably among the standards. In particular, the martensitic and ferritic steels, which contain primarily chromium as the major alloying element, were eroded less than the austenitic steels, which usually contain more than 7% nickel as well as more than 12% chromium. This is consistent with the results obtained for binary alloys, which indicate that nickel tended to increase the amount of sample eroded much more than chromium.

It would be advantageous to be able to analyze all stainless steels regardless of type with a single calibration program. Not only would preliminary sorting of unknown samples be avoided, but many specialty steels that have compositions intermediate between the common martensitic and austenitic types could be analyzed without special calibrations. However, the variability in sample erosion behavior shown in figure 14 has prevented accurate calibrations over the complete range of stainless steels when using common spark emission equipment.

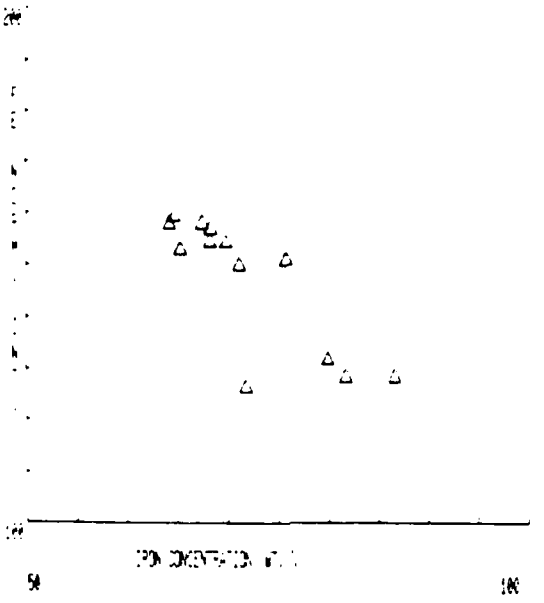

Figure 14 Normalized intensity of Fe 271 nm line versus iron concentration for some stainless steels

A common method used in spark work to account for the varying amount of material volatized from different samples is to perform what is sometimes called a "matrix dilution" calibration. If, for the i^{th} element in a sample,

$$I_i = a_i m c_i \tag{1}$$

where I_i is the intensity of emission for the i^{th} element, m is the amount of material eroded; c_i is the concentration of the element in weight percent; and a_i is a constant of proportionality; and a suitable element exists in all samples for use as an internal standard (usually the matrix element), it is possible to construct a calibration relationship of relative intensities versus relative concentrations that is independent of m. Thus

$$\frac{c_i}{c_0} = \frac{a_0}{a_i} \frac{I_i}{I_0} \tag{2}$$

where c_0, a_0, and I_0 refer to the concentration, proportionality constant, and intensity of the internal standard element. Once calibration relations like equation (2) are developed for each element in the sample, it is possible to determine the absolute concentrations in an unknown by determining the relative concentrations through the use of measured relative intensities and equation (2), and by making use of the relation

$$100 = c_0 + c_0 \sum \frac{c_i}{c_0} \tag{3}$$

to solve for c_0. Once c_0 is determined, the absolute concentrations are determined simply by multiplying the relative concentrations by c_0. For this technique to work, three conditions must hold. First, the intensity to concentration dependence must be linear, as in equation (1). Second, any background intensity must either be negligible or subtracted out beforehand. Finally, the right-hand side of equation (3) must account for all of the elements in the sample, or at least 99% of the sample composition, if 1% accuracy is desired.

When this matrix dilution method is applied to the analysis of a material such as stainless steel with a conventional spark source, it usually fails, since the calibration curves are not linear. Because of the greater linearity of calibration relations for the CSN-ICP system, it was felt that a matrix dilution calibration might work for stainless steels, using the CSN-ICP.

Figures 15 and 16 show calibration plots for nickel and chromium generated by using the same stainless steel standards as in figure 14. Emission intensities relative to the Fe-271-nm line are plotted versus the concentration of the element divided by the concentration of iron in the sample and multiplied by 100. The matrix dilution corrections seem quite effective here, since, despite the widely varying amounts of material eroded from the different samples, the calibration curves are very linear, with scatter determined largely by the repeatability of the emission intensity measurements. It is important that these major elements be determined with good accuracy, since they make up the largest part of the sumation in equation 3. Significant errors in the concentrations of the major elements would lead to inaccurate concentrations for the rest of the elements as well. Good linear calibrations were also obtained for manganese, silicon, copper, molybdenum, cobalt, niobium, and titanium. Thus the CSN-ICP can be used to analyze all ranges of stainless steels for most of the elements of interest. An important element that cannot be determined in the CSN-ICP at the concentrations of interest for most stainless steels is carbon. This is because of a high carbon background intensity in the ICP torch.

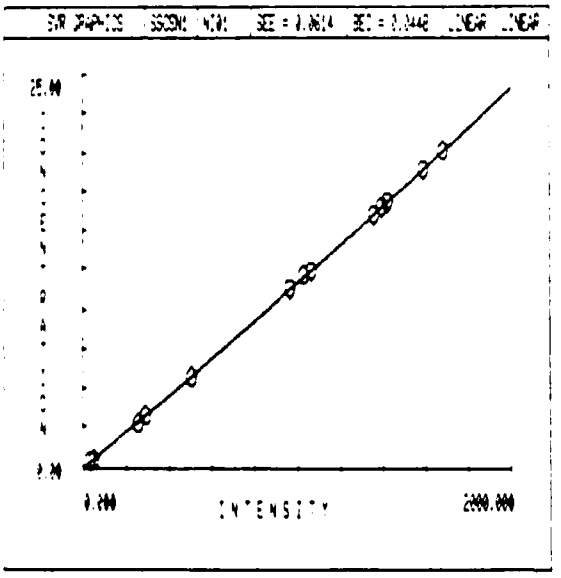

Figure 15. Calibration curve for nickel in stainless steel, using CSN-ICP and matrix dilution-style calibration.

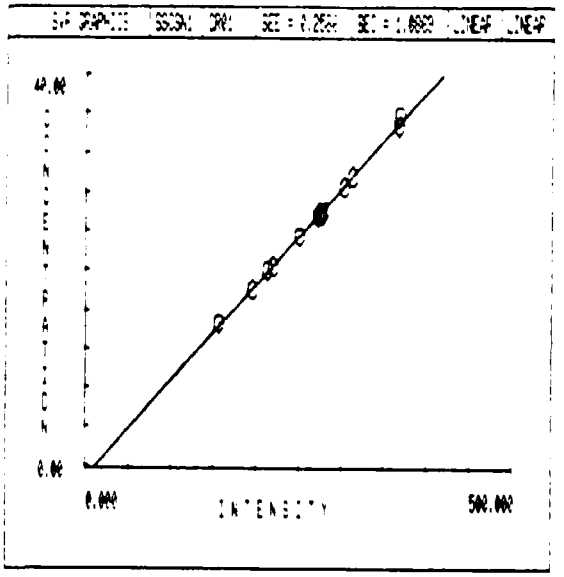

Figure 16. Calibration curve for chromium in stainless steel, using CSN-ICP and matrix dilution-style calibration.

CONCLUSIONS

The most surprising result of this work is that the enthalpies of vaporization are not the determining factor in the amount of material eroded in medium-voltage sparks. The melting behavior of the alloys seems to have a more significant effect on the amount of material eroded. Perhaps, instead of direct vaporization, the mechanism of erosion involves the mechanical sputtering of molten metal into the aerosol. However, in a standard spark source, for which both erosion and excitation occur simultaneously, the sample eventually must be vaporized to give an atomic emission signal. While it might be expected that melting would not play such a significant role for standard spark sources as the CSN-ICP measurements here would indicate, comparative measurements of iron emission signals from iron-nickel and iron-chromium alloys, using a standard spark system, yield results similar to those observed in this work: the chromium alloys show much less iron intensity than nickel alloys with the same iron concentration.[3] The important factor may be the amount of material present in the discharge gap, where vaporization and excitation take place. The sputtering of material into the gap, and thus the melting behavior, would then be important even in a standard spark stand.

The copper-zinc alloy results show that effects other than melting behavior must be important for aerosol generation, but the identity of these effects could not be determined.

The results of the CSN-ICP stainless steel calibration indicate that, even though the causes of variation in the amount of material eroded are not completely understood, they can be corrected by a simple intensity ratio and matrix dilution calculation procedure when linear calibration curves are produced. The calibration yielded superior analysis results for the main elements of stainless steels of widely varying composition. The use of CSN-ICP, rather than standard spark analysis equipment, for the examination of highly alloyed materials is recommended.

REFERENCES

1. NOSC TR 1078, *Comprehensive Chemical Analysis of Metal Alloys by Means of Inductively Coupled Plasma Optical Emission Spectroscopy*, by W.E. Glad, October 1985.
2. Hultgren, Ralph, et al., *Selected Values of the Thermodynamic Properties of Binary Alloys*, American Society for Metals, Metals Park, OH, 1973.
3. Slickers, K., *Automatic Emission Spectroscopy*, Bruhlsche Universitätsdruckerei, D-300 Giessen, Germany, 1980.

END

DATE

FILMED

5-88

DTIC